Journal of Statistical Physics, Vol. 88, Nos. 1/2, 1997

Long-Time Tails of the Velocity Autocorrelation Functions for the Triangular Periodic Lorentz Gas

H. Matsuoka[1] and R. F. Martin, Jr.[1]

Received October 12, 1995; final January 22, 1997

We present numrical results on the velocity autocorrelation function (VACF) $C(t) = \langle \mathbf{v}(t) \cdot \mathbf{v}(0) \rangle$ for the periodic Lorentz gas on a two-dimensional triangular lattice as a function of the radius R of the hard disk scatterers on the lattice. Our results for the unbounded horizon case ($0 < R < \sqrt{3}/4$) confirm $1/t$ decay of the VACF for long times (out to 100 times the mean free time between collisions) and provide strong support for the conjecture by Friedman and Martin that the $1/t$ decay is due to long free paths along which a moving particle does not scatter up to time t. Even after new sets of long free paths become available for $R < 1/4$, we continue to find good agreement between numerical results and an analytically estimated $1/t$ decay. For the bounded horizon case ($\sqrt{3}/4 \leqslant R \leqslant 0.5$), our numerical VACFs decay exponentially, although it is difficult to discriminate among pure exponential decay, exponential decay with prefactor, and stretched exponential decay.

KEY WORDS: Periodic Lorentz gas; velocity autocorrelation functions; long-time tails; billiards; diffusion coefficients; ergodic theory; chaos.

1. INTRODUCTION

The periodic Lorentz gas consists of non-interacting point particles moving freely between successive elastic collisions with fixed d-dimensional hard spheres (hard disks in two dimensions) arranged on a periodic lattice. It is a model for the diffusion of light particles through a crystal lattice. Its simple dynamics based on free inertial motion and elastic reflections off the hard spheres has thus far allowed for both analytical[1–3,15,16,18] and numerical studies.[4–7,9–14,17]

[1] Department of Physics, Illinois State University, Normal, Illinois 61790-4560.

0022-4715/97/0700-0081$12.50/0

A principal goal in the study of the Lorentz gas is to understand the connection between the dynamics of its constituent particles and its statistical properties. The main question is how its statistical, equilibrium or non-equilibrium, properties emerge from the motion of the particles. The proofs of its K-property[1] and Bernoulli-property[2] have significantly contributed to our understanding of this connection. The study of the Lorentz gas has also helped us gain more insight into non-equilibrium diffusion processes and their relation to an equilibrium statistical quantity, namely, the velocity autocorrelation function (VACF). In this paper, we will present extensive numerical results on the VACFs of the two-dimensional Lorentz gas, where hard disks are arranged on a triangular lattice. Our main focus will be on the long time decay of the VACFs.

This paper is organized as follows. In Section 2, we review previous work, both analytical and numerical, on the VACF of the two-dimensional periodic Lorentz gas. In Section 3, after defining our goals, we present our numerical results, and discuss their significance. Finally, Section 4 summarizes our findings and poses some questions for the future.

2. PREVIOUS WORK

Unless stated otherwise, all the results discussed below are for the two-dimensional periodic Lorentz gas on a square or triangular lattice, where the lattice constant is always set to one while R denotes the radius of the hard disk scatterers. We also assume that the speed $\|\mathbf{v}(t)\|$ of the moving particle remains constant and is set to unity.

According to the Einstein–Green–Kubo formula,[2] the diffusion coefficient D is related to the VACF $C(t) = \langle \mathbf{v}(t) \cdot \mathbf{v}(0) \rangle$ by

$$D = \lim_{t \to \infty} \frac{1}{4t} \langle |\mathbf{r}(t) - \mathbf{r}(0)|^2 \rangle \tag{2.1}$$

$$= \lim_{t \to \infty} \left\{ 2 \int_0^t du\, C(u) - \frac{2}{t} \int_0^t u\, du\, C(u) \right\} \tag{2.2}$$

where $\mathbf{r}(t)$ and $\mathbf{v}(t)$ are the position and velocity vectors at time t of the moving particle, and $\langle\ \rangle$ is a statistical (or microcanonical ensemble) average over all possible initial conditions for the particle. The particle

[2] Without using linear response theory, one can derive this formula directly from the relationship between the position vector $\mathbf{r}(t)$ and the velocity vector $\mathbf{v}(t)$ (i.e., $\mathbf{r}(t) - \mathbf{r}(0) = \int_0^t du\, \mathbf{v}(u)$) and a time-translational symmetry of the VACF. For more details, see ref. 12.

starts out from a position inside a Wigner–Seitz cell of the lattice with an initial velocity pointing in any possible direction. $\langle \mathbf{v}(t) \cdot \mathbf{v}(0) \rangle$ is then defined as

$$\langle \mathbf{v}(t) \cdot \mathbf{v}(0) \rangle = N \int_{-\pi/2}^{\pi/2} d\phi \cos\phi \int_0^{2\pi} dr \int_0^{\tau(r,\phi)} du\, \mathbf{v}_{(r,u,\phi)}(t) \cdot \mathbf{v}_{(r,u,\phi)}(0) \quad (2.3)$$

where (r, u, ϕ) are the coordinates for an initial condition: (r, u) specifies an initial position and ϕ an initial velocity direction (refer to Section 3.2 for more detail).

Since the diffusion coefficient D is defined in the limit where time t goes to infinity, the behavior of the VACF for large t is critical for determining D. For example, if the VACF decays as $1/t$ at long times, then the first integral in (2.2) diverges logarithmically and gives an infinite value to D, whereas if the VACF decays exponentially, both integrals in (2.2) yield finite values and D is well defined. This long-time behavior of the VACF is the main focus of this paper.

When we discuss the statistical properties of the periodic Lorentz gas, a geometrical feature of the lattice called "horizon" becomes important. The Lorentz gas behaves differently when it has a "bounded (or finite) horizon" or an "unbounded (or infinite) horizon." A lattice has an unbounded horizon if there exist particle trajectories of infinite length along which a particle can travel through the lattice without ever colliding with any hard disk. For example, the square Lorentz gas has an unbounded horizon if the diameter of the disks is smaller than the lattice constant (i.e., $0 < R < 0.5$). For the triangular Lorentz gas, there exists a critical value $R_c = \sqrt{3}/4$ for the radius of the disks that separates the unbounded horizon case ($0 < R < R_c$) from the bounded horizon case ($R_c \leqslant R \leqslant 0.5$).

2.1. The Bounded Horizon Case

2.1.1. Analytical Results. Not much is known rigorously about the VACF for either the bounded or unbounded horizon case. However, Bunimovich and Sinai, and later Bunimovich, Sinai and Chernov[3] obtained the following stretched exponential bound for a different type of velocity autocorrelation function $E\{\mathbf{v}(n), \mathbf{v}(0)\}$ (hereafter the velocity n-correlation function or VNCF), which is a function of the number of collisions n instead of time t:

$$|E\{\mathbf{v}(n), \mathbf{v}(0)\}| \leqslant A \exp(-\kappa n^{\nu}) \quad (2.4)$$

where A and κ are positive constants and $1/2 \leqslant \gamma \leqslant 1$. The VNCF is defined as

$$E\{\mathbf{v}(n), \mathbf{v}(0)\} = \frac{1}{4\pi R} \int_{-\pi/2}^{\pi/2} d\phi \cos\phi \int_0^{2\pi R} dr\, \mathbf{v}_{(r,\phi)}(n) \cdot \mathbf{v}_{(r,\phi)}(0) \tag{2.5}$$

where the inner product $\mathbf{v}_{(r,\phi)}(n) \cdot \mathbf{v}_{(r,\phi)}(0)$ between the velocity $\mathbf{v}_{(r,\phi)}(n)$ after the nth collision and the initial velocity $\mathbf{v}_{(r,\phi)}(0)$ is averaged over all possible initial conditions for the particle starting on the perimeter (or circle) of a hard disk. Here r specifies an initial position along the circle, and ϕ the angle between the direction of the initial velocity and the normal to the circle at the initial position.

The average (2.5) is different from the average defined in (2.3) in two respects. First, in (2.5) the average is taken over initial conditions only on the perimeter of a disk, whereas in (2.3) the average is taken over initial conditions inside the Wigner–Seitz cell. Second, in (2.5) we are concerned with the velocity of the particle after the nth collision, while in (2.3) we are interested in the velocity $\mathbf{v}_{(r,u,\phi)}(t)$ at time t, which is not simply related to $\mathbf{v}_{(r,\phi)}(n)$. Because of these differences, there is no simple relationship between the VNCF and the VACF and hence no rigorous upper bound for the VACF has been established. The bound (2.4) is, however, consistent with a finite value for the diffusion coefficient, and Bunimovich and Sinai[3] indeed proved that for a periodic Lorentz gas with a bounded horizon the diffusion coefficient exists and is finite. This in turn implies that the VACF for this case must decay faster than $1/t$.

2.1.2. Numerical Results: Overlapping Disk Case. A stretched exponential decay of an n-correlation function was found numerically by Casati, Comparin, and Guarneri[4] for a square Lorentz gas with mutually overlapping disks of radius $R = \sqrt{5}/4 > 0.5$. This system has a bounded horizon: the particle is, in fact, trapped inside a region bounded by four disks and does not diffuse throughout the lattice. The diffusion coefficient is therefore vanishing. The n-correlation function $\rho(n)$ studied by Casati, Comparin, and Guarneri is not the VNCF of (2.5) but was found to behave as

$$\rho(n) \sim C \exp(-1.4 n^{0.42}) \tag{2.6}$$

Since Bunimovich, Sinai, and Chernov[3] proved the bound (2.4) for any n-correlation function, this result (2.6) is not consistent with their bound.

Recently, Garrido and Gallavotti[5] numerically obtained the VNCF for the square Lorentz gas with $R = \sqrt{5}/4$ but concluded that their data was not good enough to distinguish between exponential and stretched

exponential decays. The long-time decay of the VNCF for the square Lorentz gas with $R > 0.5$ therefore remains an open question. Garrido and Gallavotti also calculated the VACF for the same case and their results support either purely exponential decay or stretched exponential decay with a stretched exponent of 0.995.

2.1.3. Numerical Results: Non-overlapping Disk Case.

2.1.3.A. The VNCF. For the triangular Lorentz gas, the horizon is bounded if $\sqrt{3}/4 \leqslant R \leqslant 0.5$. Machta and Reinhold[6] numerically studied the VNCF in this case and found it to behave as

$$E\{\mathbf{v}(n), \mathbf{v}(0)\} \sim (-1)^n A \exp(-\lambda n) \qquad (\text{for } \sqrt{3}/4 \leqslant R < 0.5) \tag{2.7}$$

where A is a positive constant and

$$\lambda = \frac{1 - 2R + \sqrt{1 - 2R}}{R} \tag{2.8}$$

where λ goes to zero as R approaches 0.5. A similar exponential decay of the VNCF was observed by Garrido and Gallavotti[5] in the square Lorentz gas with two sublattices of hard disks of two different sizes.

At $R = 0.5$, where three adjacent disks touch each other, Machta and Reinhold found that

$$E\{\mathbf{v}(n), \mathbf{v}(0)\} \sim (-1)^n \frac{B}{n} \qquad (\text{at } R = 0.5) \tag{2.9}$$

where $B \sim 0.675$. Machta[7] had previously argued that this $1/n$ decay is largely due to a series of successive collisions of the particle with two adjacent disks. The slow $1/n$ decay then reflects a highly correlated nature of these collisions, analogous to the collisions between the parallel boundaries in a stadion as pointed out by Vivaldi, Casati, and Guarneri.[8]

A similar $1/n$ decay was observed by Bouchaud and Le Doussal[9] for the square Lorentz gas with $R = 0.5$, where four adjacent disks are tangent to each other. In this case, the VNCF was found to behave as

$$E\{\mathbf{v}(n), \mathbf{v}(0)\} \sim (-1)^n \frac{B'}{n} \tag{2.10}$$

where $B' = 0.9 \pm 0.1$ which is very close to $4B/3$ as we expect from a geometrical difference between the two lattices (i.e., four, instead of three, corners in a region bounded by four disks).

Machta and Reinhold also found the following scaling form to fit both (2.7) and (2.9):

$$E\{\mathbf{v}(n), \mathbf{v}(0)\} \sim (-1)^n \frac{f(\lambda n)}{n} \tag{2.11}$$

where $f(x) \to B$ as $x \to 0$ and $f(x) \to Cx \exp(-x)$ with $C \sim 4/\pi$ as $x \to \infty$. Based on this scaling form, they suggested that the approach toward $R = 0.5$ may be regarded as a type of second-order phase transition, as also pointed out by Bouchaud and Le Doussal,[9,10] with $1/\lambda$ as a correlation "length" which diverges at $R = 0.5$.

2.1.3.B. The VACF. Through a numerical study of VACFs, Friedman and Martin[11,12,13] found that for the triangular Lorentz gas with a bounded horizon, the VACF decays roughly exponentially. They also conjectured[12] that the VACF may have a pre-factor of $t^{-1/2}$:

$$C(t) \sim t^{-1/2} \exp(-At)\, F(t) \tag{2.12}$$

where $F(t)$ is an oscillatory function of t and A is related to the maximal Lyapunov exponent. We shall present some additional results on this exponential decay in Section 3.3.2.

Garrido and Gallavotti[5] found that for the square Lorentz gas with two sublattices of hard disks of different sizes, the VACF decays roughly exponentially and that the decay rate is apparently uncorrelated to the maximal Lyapunov exponent.

2.2. The Unbounded Horizon Case

2.2.1. Analytical Results. For the Lorentz gas with an unbounded horizon, Bunimovich[15] argued that the VNCF is also bounded by a stretched exponential as in (2.4) with possibly different values for A, κ, and γ. Bunimovich, Sinai and Chernov[3] then proved that $1/2 \leqslant \gamma \leqslant 1$.

Recently Bleher[16] has shown that under some natural assumptions on the free motion vector autocorrelation function, the limit distribution of the particle displacement

$$\lim_{t \to \infty} \frac{\mathbf{r}(t) - \mathbf{r}(0)}{(t \ln t)^{1/2}} \tag{2.13}$$

is a Gaussian. This result is based on some conjectures and therefore not completely proven, but it is consistent with a $1/t$ decay for the VACF, and the diffusion coefficient D defined in (2.1) would be then infinite.

2.2.2. Numerical Results: Triangular Lorentz Gas. Based on a numerical study, Friedman and Martin[11,12,13] proposed that for the triangular Lorentz gas with an unbounded horizon, the VACFs decay as $1/t$ for large t. In the unbounded horizon case, for any time t, there exists a group of trajectories along which the moving particle never collides with any hard disk up to t. Friedman and Martin argued that these trajectories, or long free paths, are responsible for the $1/t$ decay. In fact, the $1/t$ dependence comes from the volume of a region in the phase space corresponding to these trajectories. Based on this argument, Friedman and Martin[12,13] derived an analytical formula for the $1/t$ decay (see Section 3.3.3), and the VACFs numerically obtained by Friedman and Martin[12,13] appeared to approach the behavior given by this formula. However, the agreement between the numerical results and this formula was not conclusive mainly because of the relatively short time range (up to $t = 25\tau$, where τ is the mean free time which will be defined in Section 3.3) over which the VACFs were calculated.

In Section 3, we will provide further numerical evidence to support this $1/t$ decay by extending the time range up to $t = 100\tau$ so that an asymptotic behavior of the VACF can be examined. To probe into longer times, we choose smaller values for R, for which the values of the VACFs stay far above their noise level even at long times. If the VACF decays as $1/t$ and is not oscillatory, then the diffusion coefficient should diverge for the triangular Lorentz gas with an unbounded horizon. We will also provide a numerical evidence for this divergence of the diffusion coefficient in Section 3.3.3.

2.2.3. Numerical Results: Square Lorentz Gas.

2.2.3.A. The VNCF. For the square Lorentz gas with $R < 0.5$, Bouchaud and Le Doussal[9] found the VNCF to decay as a stretched exponential:

$$E\{\mathbf{v}(n), \mathbf{v}(0)\} \sim (-1)^n \exp(-\kappa n^\gamma) \tag{2.14}$$

where $\gamma = 0.86 \pm 0.06$, $\log \kappa = -0.27$ (for $R = 0.5$), and $\log \kappa = -0.2$ (for $R = 0.05$). This result is consistent with Bunimovich, Sinai, and Chernov's finding,[3] $1/2 \leqslant \gamma \leqslant 1$. The exponent γ was found to be independent of R. Garrido and Gallavotti[5] also found that for the square Lorentz gas with $R = 7\sqrt{2}/40$, the VNCF decays exponentially with different decay rates for even and odd values of n.

2.2.3.B. The VACF. Friedman[12] presented numerical results which suggest that the VACF for the square Lorentz gas with $R = 0.4$ (< 0.5) decays as $1/t$ as in the triangular Lorentz gas with an unbounded horizon.

Furthermore, Zacherl *et al.*[17] numerically obtained the power spectrum $S(\omega)$ of the VACF for $R=0.05$ and 0.225, and found $S(\omega)$ to behave as $|\ln \omega|$ for small ω or low frequencies, consistent with a $1/t$ decay in the VACF. Using a random walk approximation, they also derived a $1/t$ decay for the VACF and a $t \ln t$ divergence for the mean square displacement $\langle |\mathbf{r}(t)-\mathbf{r}(0)|^2 \rangle$ for large t. Garrido and Gallavotti[5] also found that for the square Lorentz gas with $R=7\sqrt{2}/40$, the VACF decays exponentially for short times up to $t=16\tau$.

3. NEW RESULTS

3.1. Goals

From the above review of previous work, it is clear that the issue of the long time tails of the VACFs for the periodic Lorentz gas in two dimensions is yet to be settled. In particular, the $1/t$ decay for the unbounded horizon case has been neither rigorously proved nor conclusively supported by numerical evidence. Even for the bounded horizon case, we do not know with certainty whether the long time decay of the VACF is pure exponential, exponential with a $t^{-1/2}$ prefactor, or stretched exponential. It is the main goal of this paper to numerically examine the long time decay of the VACF for the triangular Lorentz gas in both the bounded and unbounded horizon case. The main questions to be addressed are:

(i) For the bounded horizon case, does the VACF decay as pure exponential, exponential with a $t^{-1/2}$ prefactor, or stretched exponential?

(ii) For the unbounded horizon case, does the VACF decay as $1/t$? If so, then is the $1/t$ decay due to the long free paths? More specifically, does the VACF follow the analytical formula given by Friedman and Martin?

3.2. Numerical Method

We calculated the VACF by numerically evaluating the right hand side of

$$\langle \mathbf{v}(t) \cdot \mathbf{v}(0) \rangle = N \int_{-\pi/2}^{\pi/2} d\phi \cos\phi \int_0^{2\pi} dr \int_0^{\tau(r,\phi)} du\, \mathbf{v}_{(r,u,\phi)}(t) \cdot \mathbf{v}_{(r,u,\phi)}(0) \quad (3.1)$$

where the integral is taken over all initial conditions (r, u, ϕ) for the moving particle and $\mathbf{v}_{(r,u,\phi)}(t)$ is its velocity at time t. Initial positions are

uniformly selected from a Wigner–Seitz cell (for the triangular lattice, it is a hexagon) except for the interior of the hard disk at the center. The directions of initial velocities are also uniformly chosen from all the possible directions of motion starting from each initial position. The speed $\|\mathbf{v}(t)\|$ of the particle is always set to unity. The coodinates (r, u, ϕ) are chosen as follows. Starting from an initial position, extend the velocity vector backwards until the vector hits the disk. At each side of the hexagon, periodic boundary conditions are assumed so that the particle reenters at the opposite side of the cell. The position r then specifies the location of the point of intersection measured in radians from a fixed point on the circle, u is the distance between the initial position and the point of intersection (or the time from the last collision up to the initial position, since the speed of the particle is unity), and ϕ is the angle between the velocity vector and the normal to the circle at the point of intersection. r varies from 0 to 2π, u from 0 to $\tau(r, \phi)$ which is the time when the particle starting on the circle with an initial condition (r, ϕ) collides with another disk, and ϕ from $-\pi/2$ to $\pi/2$. With these coordinates (r, u, ϕ), the Liouville measure in the phase space is given by $N \cos\phi \, d\phi \, dr \, du$, where N is a normalization factor.

After a change of varables $(x = \sin\phi)$ and exploiting the 6-fold rotational symmetry of the hexagon, (3.1) becomes

$$\langle \mathbf{v}(t) \cdot \mathbf{v}(0) \rangle = \tilde{N} \int_{-1}^{1} dx \int_{0}^{\pi/6} dr \int_{0}^{\tau(r,\phi)} du \, \mathbf{v}_{(r,u,x)}(t) \cdot \mathbf{v}_{(r,u,x)}(0) \tag{3.2}$$

where $\tilde{N} = (6R/\pi)(\sqrt{3}/2 - \pi R^2)^{-1}$. Since $\mathbf{v}_{(r,u,x)}(0)$ is independent of u (*i.e.*, $\mathbf{v}_{(r,u,x)}(0) = \mathbf{v}_{(r,x)}(0)$), we can take $\mathbf{v}_{(r,x)}(0)$ outside the innermost integral, and then using both the fundamental theorem of calculus and

$$\mathbf{v}_{(r,u,x)}(t) = \mathbf{v}_{(r,0,x)}(t+u) = d\mathbf{r}_{(r,0,x)}(t+u)/dt = d\mathbf{r}_{(r,0,x)}(t+u)/du \tag{3.3}$$

we obtain

$$\langle \mathbf{v}(t) \cdot \mathbf{v}(0) \rangle = \tilde{N} \int_{-1}^{1} dx \int_{0}^{\pi/6} dr \, \mathbf{v}_{(r,x)}(0) \cdot \{\mathbf{r}_{(r,0,x)}(t + \tau(r, x)) - \mathbf{r}_{(r,0,x)}(t)\} \tag{3.4}$$

Using this formula, the VACFs were calculated numerically by replacing the double integral with a discrete sum over $4500^2 (= 2.025 \times 10^7)$ (for a few cases, $10000^2 (= 1 \times 10^8)$) initial conditions uniformly selected from a regular grid in r-x plane. The computer program is written in double precision FORTRAN, and generates trajectories for the particle with different

initial conditions by calculating the discrete T-map which takes the particle from one collision with a hard disk to the next exactly.[3]

3.3. Numerical Results

All the VACFs will be presented as functions of time t measured in units of the mean free time τ, which is defined as

$$\tau = \frac{1}{4\pi} \int_0^{2\pi} dr \int_{-\pi/2}^{\pi/2} d\phi \cos\phi \tau(r, \phi) \tag{3.5}$$

Using

$$R \int_0^{2\pi} dr \int_{-\pi/2}^{\pi/2} d\phi \cos\phi \tau(r, \phi) = R \int_0^{2\pi} dr \int_{-\pi/2}^{\pi/2} d\phi \cos\phi \int_0^{\tau(r,\phi)} du$$

$$= 2\pi \left(\frac{\sqrt{3}}{2} - \pi R^2 \right) \tag{3.6}$$

where $2\pi(\sqrt{3}/2 - \pi R^2)$ is the volume of the phase space, we find

$$\tau = \frac{1}{2R} \left(\frac{\sqrt{3}}{2} - \pi R^2 \right) \tag{3.7}$$

When we compare the VACFs for different values of R, we must keep in mind that τ increases as R decreases so that a faster decay of a VACF as a function of t/τ may not necessarily mean a faster decay in real time t.

We have calculated each VACF $C(t)$ for t that is an integer multiple of $\tau/8$. We have chosen the values for the disk radius R to be 0.499, 0.48, and 0.44 for the bounded horizon case, and 0.4329, 0.42, 0.41, 0.4, 0.35, 0.3, 0.2, 0.17, 0.16, and 0.125 for the unbounded horizon case (*cf.* the crossover radius $R_c = \sqrt{3}/4 = 0.4330$). To avoid redundancy, we will show our results only for $R = 0.499$, 0.48, 0.44, 0.4329, 0.42, 0.4, 0.3, 0.2, 0.17, and 0.125 in this paper.

All the computations were done on IBM RS6000 computers. The CPU time for calculating a VACF up to $t = 100\tau$ depended rather strongly on the value of R (it was between 132 hours ($R = 0.499$) and 185 hours ($R = 0.16$) with an average of 150 hours).

[3] Details of the algorithm for the T-map are given in ref. 12, though we have rewritten the program extensively to reduce the computation time.

3.3.1. Roundoff Errors and Statistical Uncertainty. As Friedman and Martin[13] have shown, round-off errors due to our algorithm based on the discrete T-map are negligible and a main source of numerical error is the finite number of initial conditions. Note that the T map is an analytically exact map that maps a point where the particle collides with the disk to another such point for the next collision and, unlike numerical integration of a differential equation, introduces only negligible amount of roundoff errors for a typical length of the particle trajectories that we calculated using double precision. We expect the statistical uncertainty due to the finite number of initial conditions to be roughly $1/\sqrt{4500^2} \sim 2.2 \times 10^{-4}$ (or $1/\sqrt{10000^2} \sim 1 \times 10^{-4}$), where 4500^2 (or 10000^2) is the number of the initial conditions we used. As we will show below, this estimate is close to the actual noise level ($\sim 3-4\times 10^{-4}$) found in the calculated VACFs. This further corroborates that the main source of numerical error is the finite number of initial conditions.

3.3.2. The Bounded Horizon Case: $\sqrt{3}/4 \leqslant R \leqslant 0.5$. Figure 1 shows $|C(t)|$ for 10000^2 initial conditions. The envelope of the VACF decays exponentially up yo $t \sim 30\tau$. In this range, the VACF also oscillates alternately between positive and negative values with a period of roughly 7τ. Beyond $t \sim 40\tau$, the VACFs calculated with 4500^2 and 10000^2 initial conditions oscillate randomly around zero (see Fig. 2 for 10000^2 initial conditions) with a maximum amplitude of $\sim 2-4\times 10^{-4}$ and $\sim 1-3\times 10^{-4}$,

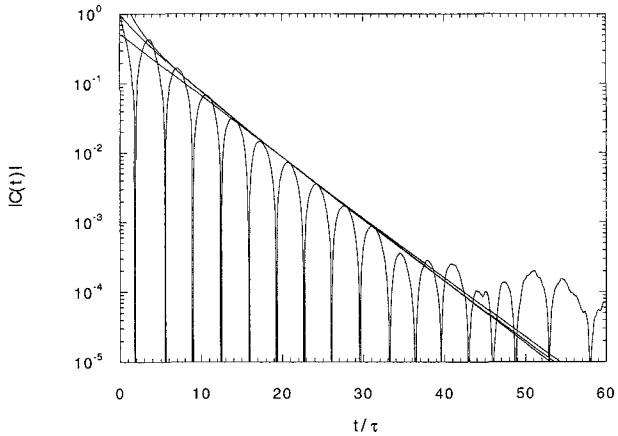

Fig. 1. Absolute value of the VACF $|C(t)|$ as a function of time in man free time units for $R = 0.499$ with 1×10^8 initial conditions sampled. Three different fits to the maxima of $|C(t)|$ are also plotted. They are, from the top, $1.52(t/\tau)^{-1/2}\exp\{-0.183(t/\tau)\}$ (exponential with prefactor), $\exp\{-0.32(t/\tau)^{0.9}\}$ (stretched exponential), and $0.525\exp\{-0.205(t/\tau)\}$ (pure exponential).

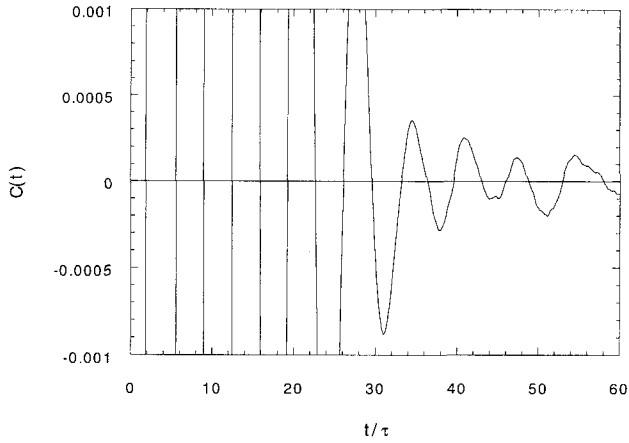

Fig. 2. The VACF $C(t)$ as a function of time in mean free time units for $R = 0.499$ with 1×10^8 initial conditions sampled.

respectively, which are close to our estimated statistical uncertainty of $1/\sqrt{4500^2} \sim 2.2 \times 10^{-4}$ and $1/\sqrt{10000^2} \sim 1 \times 10^{-4}$, respectively. Therefore, the VACFs beyond $t \sim 40\tau$ are completely drowned by statistical uncertainty.

The origin of the periodic oscillation up to $t \sim 40\tau$ was discussed by Friedman and Martin[13] who suggested that this oscillation is similar to that found in the VACF for a particle trapped in a square box. In their view, highly correlated motion inside a trapping region surrounded by three disks, also studied by Machta and Reinhold, is the cause for this periodic oscillation. Since the VACF for a square box has a $t^{-1/2}$ prefactor in front of an exponential function, they also conjectured a $t^{-1/2}$ prefactor for the VACF for the bounded horizon case.

To test whether the VACF has a $t^{-1/2}$ prefactor, we have plotted $\log\{t^{1/2}\,|C(t)|\}$ against t/τ. Although $t^{1/2}\,|C(t)|$ appears to decay exponentially over a slightly larger range in time (within an extra range between 10τ and 15τ) than $|C(t)|$ does (see Fig. 1), we can neither confirm nor reject a $t^{-1/2}$ prefactor since we do not know exactly where the asymptotic behavior for the VACF starts. To determine the presence or absence of this $t^{-1/2}$ prefactor, we must then calculate the VACF extremely accurately into further longer times, which would be virtually impossible because of its exponential decay. Even if the VACF were calculated at large t with high precision, the effect of the $t^{-1/2}$ prefactor would be almost completely masked by the exponential decay. In fact, it is easy to fit a function $t^{-1/2}\exp(-at)$ over many decades with a pure exponential $\exp(-bt)$ with b different from a.

To test whether the VACF can be fitted by a stretched exponential, we have fit $\log\{|\log|C(t)||\}$ against t/τ, yielding $\exp\{-0.32(t/\tau)^{0.9}\}$. Although this appears to better fit the numerical results over a slightly larger range in time (within an extra range between 10τ and 15τ) than by a pure exponential (see Fig. 1), we can neither confirm nor reject a stretched exponential fit since we do not know exactly where the asymptotic behavior for the VACF starts. We here face the same difficulty as when we try to distinguish between a pure exponential and an exponential with a $t^{-1/2}$ prefactor. In fact, it is easy to fit a function $\exp\{-0.32(t/\tau)^{0.9}\}$ over many decades with a pure exponential. It is therefore beyond numerical approach to discriminate among exponential decay, exponential decay with a prefactor, and stretched exponential decay and should be resolved by an analytical study.

Figure 3 shows a semi-logarithmic plot of $|C(t)|$ for $R=0.48$. Because the VACF for this case is less ordered than that for $R=0.499$, it is more difficult to fit its envelope precisely. Nevertheless, the VACF appears to decay roughly exponentially with time up to $t\sim 20\tau$. Beyond $t\sim 20\tau$, the VACF oscillates around zero as statistical uncertainty masks the VACF. Up to $t\sim 20\tau$, it can also be fitted by an exponential with a $t^{-1/2}$ prefactor. A stretched exponential decay cannot be ruled out, as well.

The envelope of the VACF for $R=0.44$, as shown in Fig. 4, also decays roughly exponentially up to $t\sim 20\tau$ without regular oscillation. We cannot rule out a $t^{-1/2}$ prefactor or a stretched exponential decay of the VACF. The VACF beyond $t\sim 20\tau$ is again dominated by statistical

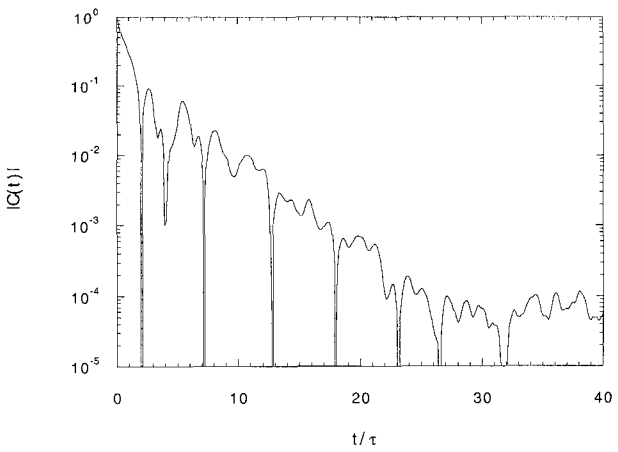

Fig. 3. Absolute value of the VACF $|C(t)|$ as a function of time in mean free time units for $R=0.48$ with 1×10^8 initial conditions sampled.

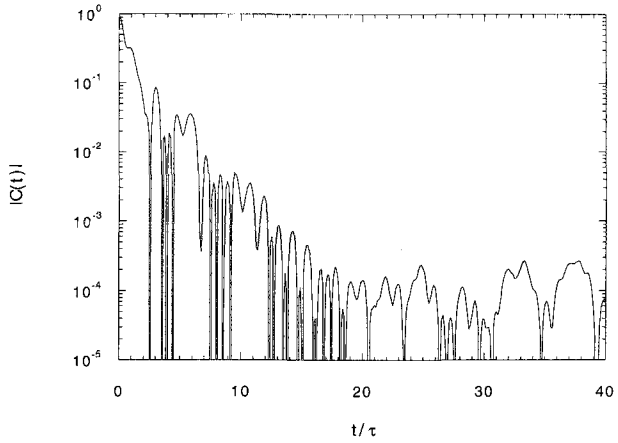

Fig. 4. Absolute value of the VACF $|C(t)|$ as a function of time in mean free time units for $R = 0.44$ with 1×10^8 initial conditions sampled.

uncertainty. Although the VACFs as functions of t/τ appear to decay faster for smaller R, the VACFs as functions of t decay more slowly for smaller R with their exponential decay rates being roughly 2.4, 2.0, and 1.4 for $R = 0.499$, 0.48, and 0.44, respectively. This is consistent with our expectation that for smaller R, the moving particle loses its past memory more slowly because of fewer collisions per unit time.

Time-dependent diffusion coefficients $D(t)$ were calculated for $R = 0.499$, 0.48, and 0.44 by numerically integrating the right hand side of (2.2) up to time t. If the integrals in (2.2) converge to finite values, then diffusion coefficient exists. Figure 5 shows the inside of the parenthesis in (2.2) as a function $D(t)$:

$$D(t) \equiv 2 \int_0^t du\, C(u) - \frac{2}{t} \int_0^t u\, du\, C(u) \tag{3.8}$$

$D(t)$ for $R = 0.499$, 0.48, and 0.44 all converge to finite values as t is increased. The flatness of the curves of $D(t)$ beyond $t \sim 35\tau$ for $R = 0.499$ and beyond $t \sim 25\tau$ for $R = 0.48$ and 0.44 supports our assumption that the VACFs in these ranges are masked by statistical uncertainty. The diffusion coefficients derived from our VACFs are completely consistent with the numerical results by Machta and Zwanzig.[14]

3.3.3. The Unbounded Horizon Case: $0 < R < \sqrt{3}/4$. Before we present our numerical results in this case, let us outline and extend the argument for the $1/t$ decay of the VACF given by Friedman and Martin.[11,12,13]

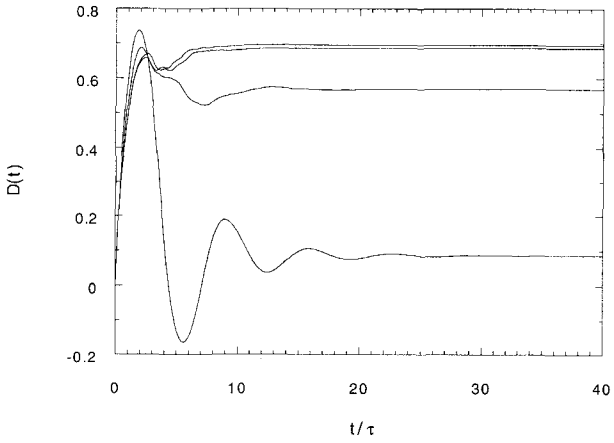

Fig. 5. Time-dependent diffusion coefficient $D(t)$ calculated from the VACFs for $R=0.499$, 0.48, 0.44, and 0.4329. Curves are, from the top at long times, for $R=0.4329$, 0.44, 0.48, and 0.499.

A crucial point is that as soon as the horizon opens up or R becomes less than $\sqrt{3}/4$, there are certain directions in the lattice along which the particle can travel without ever colliding with any of the disks. In order words, we have open channels or corridors of infinite length. For $1/4 \leqslant R < \sqrt{3}/4$, we have twelve open channels starting from a Wigner–Seitz cell. As R decreases further, more channels open up along different directions. For example, for $\sqrt{21}/28 \leqslant R < 1/4$, twelve more channels would be introduced. Because the volume of a region in the phase space associated with the long free paths in these channels varies as $1/t$, these paths contribute a $1/t$ term to the VACF at long times. For example, for $1/4 \leqslant R < \sqrt{3}/4$, Friedman and Martin[12,13] obtained

$$C_{free}^{(1)}(t) = \frac{24}{\pi} \frac{R(\sqrt{3}/4 - R)^2}{(\sqrt{3}/2 - \pi R^2)^2} \frac{\tau}{t} \tag{3.9}$$

We can extend this result to obtain a contribution to the VACF from a set of long free paths that become available for a range, $R_n \leqslant R < R_{n+1}$, where $R_n = \sqrt{3}/(4\sqrt{n^2 - n + 1})$. We can then estimate the $1/t$ decay due to all the available long free paths in $R_n \leqslant R < R_{n+1}$ to be

$$C_{free}^{(n)}(t) = \left(\sum_{i=1}^{n} F_i \right) \frac{\tau}{t} \tag{3.10}$$

where

$$F_i = \frac{24R}{\pi\sqrt{i^2-i+1}} \frac{(\sqrt{3}/4 - R\sqrt{i^2-i+1})^2}{(\sqrt{3}/2 - \pi R^2)^2} \tag{3.11}$$

Of course, there are other contributions to the VACF from other parts of the phase space, and these may cancel the contribution from the long free paths. It is however possible that the other contributions would add up to an exponential decay, and thus only the $1/t$ decay survives at sufficiently long times.

One notable point about $C_{free}^{(n)}(t)$ is that with a fixed value of t, it increases for smaller R. This means that if (3.9) and (3.10) give the actual asymptotic behavior of the VACFs, then with a smaller value of R, we have a better chance of observing the $1/t$ decay at long times, say at $t = 100\tau$, because then only the $1/t$ tail of the VACF can rise above the level of statistical uncertainty. Therefore, it is our strategy to calculate the VACF for various values of R, especially, for smaller values, and to test (3.9) as well as (3.10). By testing (3.10) as well, we will further substantiate the role of the long free paths along the open channels as the origin of the $1/t$ decay for the unbounded case.

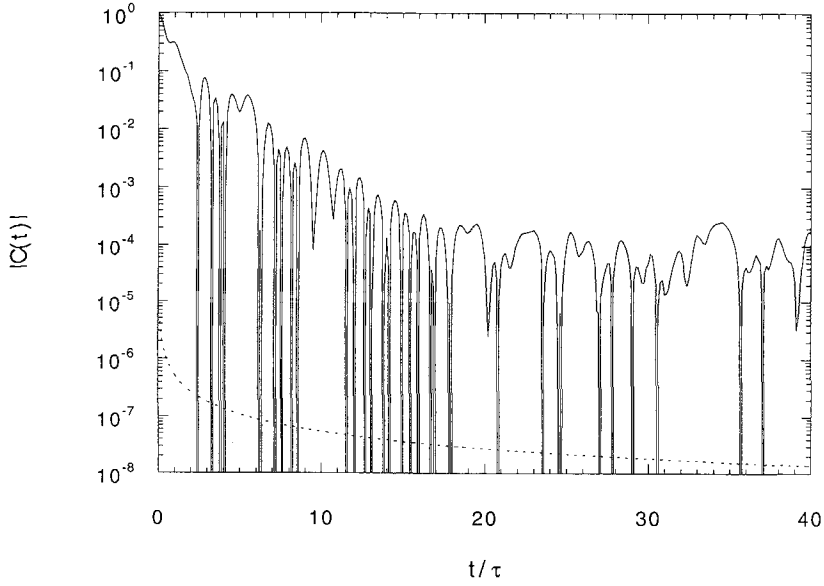

Fig. 6. Absolute value of the VACF $|C(t)|$ as a function of time in mean free time units for $R = 0.4329$ with 2.025×10^7 initial conditions sampled. The analytical estimate for the $1/t$ decay $C_{free}^{(1)}(t)$ is also plotted as a broken curve.

As another check for the $1/t$ decay, we will also plot $D(t)$ defined in (3.8) against $\log_{10}(t)$, because if the VACF decays as $1/t$, then $D(t)$ should diverge as $\ln(t)$. In studying the long time tail of the VACF for a disordered Lorentz gas, Lowe and Masters[19] found that $D(t)$ allowed them to probe into long times, where the VACF itself becomes statistically indistinguishable from zero.

3.3.3.A. 12 Open Channels: $1/4 \leqslant R < \sqrt{3}/4$. For R just below the critical value $R_c = \sqrt{3}/4$, it is very difficult to observe the $1/t$ decay in the VACF, because in this case the free-path contribution $C^{(1)}_{free}(t)$ could be much smaller than the statistical uncertainty. In fact, as shown in Fig. 6, the VACF for $R = 0.4329$ appears very similar to that for $R = 0.44$ and decays roughly exponentially with time up to $t \sim 15\tau$, beyond which the VACF oscillates around zero as statistical uncertainty masks the VACF. $D(t)$ for this case (see Fig. 5) also appears very similar to that for $R = 0.44$ and seems to converge to a finite value as t is increased. Therefore the transition between the bounded and unbounded horizon case is smooth and the emergence of the $1/t$ decay just below the critical radius is extremely difficult to detect.

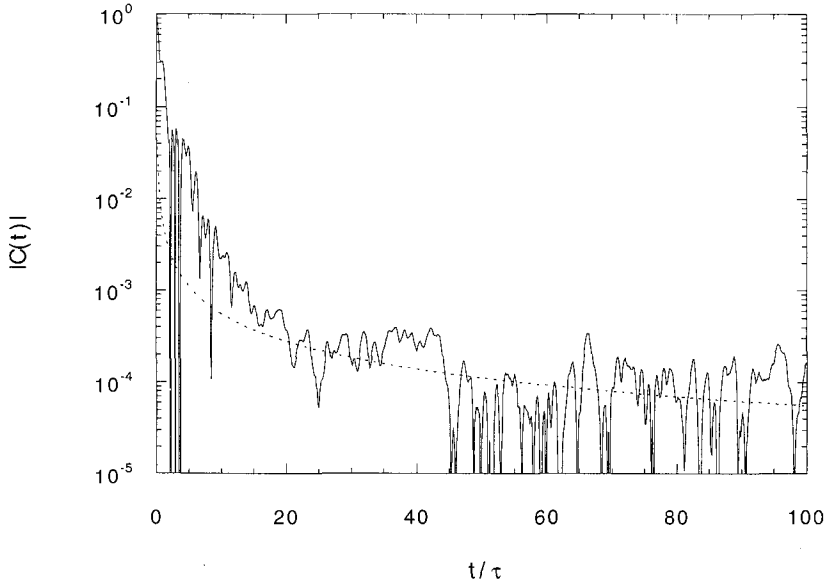

Fig. 7. Absolute value of the VACF $|C(t)|$ as a function of time in mean free time units for $R = 0.42$ with 2.025×10^7 initial conditions sampled. The analytical estimate for the $1/t$ decay $C^{(1)}_{free}(t)$ is also plotted as a broken curve.

Figure 7 shows a semi-logarithmic plot of $|C(t)|$ for $R=0.42$. The VACF initially decays roughly exponentially and then appears to follow the free-path contribution $C^{(1)}_{free}(t)$ beyond $t\sim 20\tau$, although it exhibits apparently random fluctuations beyond $t\sim 40\tau$. However, the VACF fluctuates about $C^{(1)}_{free}(t)$ rather than around zero (see Fig. 8). This is different from the bounded horizon case, where the VACFs fluctuate around zero at long times because of statistical uncertainty (see Fig. 2). Although the size of $C^{(1)}_{free}(t)$ is close to that of statistical uncertainty, this behavior of the VACF nevertheless suggests the $1/t$ decay. Figure 10 shows that $D(t)$ varies linearly in $\log_{10}(t)$ beyond $t\sim 20\tau$, which adds further support for the $1/t$ decay.

As discussed above, we should have a better chance of confirming the $1/t$ decay if we explore even smaller values of R. This has proven to be the case for the VACFs for $R=0.41$, 0.4, 0.35, and 0.3. Figure 9 shows the VACF for $R=0.3$ as a representative case. The VACFs for $R=0.41$, 0.4, 0.35, and 0.3 all follow $C^{(1)}_{free}(t)$ given by (3.9). Statistical fluctuations around $C^{(1)}_{free}(t)$ are, in all the cases, roughly $\sim 3-4\times 10^{-4}$ at most, which is consistent with the results for other values of R. $D(t)$ also diverges linearly with $\log_{10}(t)$ in all the cases (see Fig. 10).

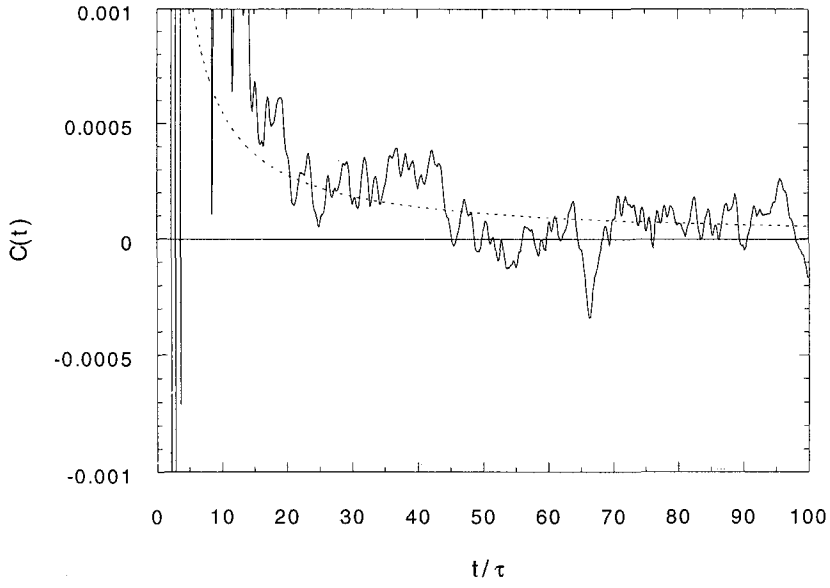

Fig. 8. The VACF $C(t)$ as a function of time in mean free time units for $R=0.24$ with 2.025×10^7 initial conditions sampled. The analytical estimate for the $1/t$ decay $C^{(1)}_{free}(t)$ is also plotted as a broken curve.

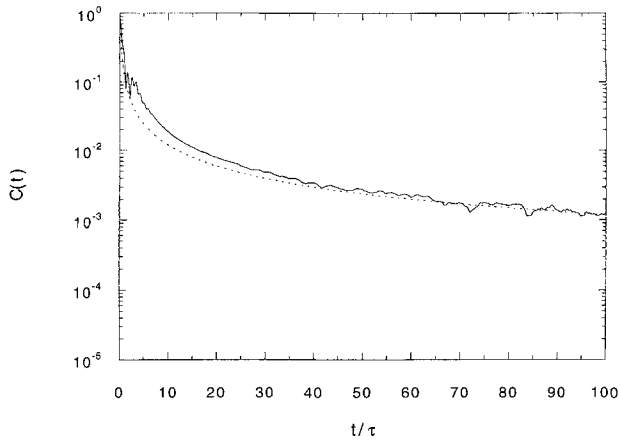

Fig. 9. The VACF $C(t)$ as a function of time in mean free time units for $R = 0.3$ with 2.025×10^7 initial conditions sampled. The analytical estimate for the $1/t$ decay $C^{(1)}_{free}(t)$ is also plotted as a broken curve.

3.3.3.B. 24 Open Channels: $\sqrt{21}/28 \leqslant R < 1/4$. For $\sqrt{21}/28 \leqslant R < 1/4$, we have two sets of twelve open channels, and Fig. 11 shows that the VACFs for $R = 0.17$ follows $C^{(2)}_{free}(t)$ given by (3.10) beyond $t \sim 60\tau$. Figure 10 also shows that in this range of time $D(t)$ diverges linearly with $\log_{10}(t)$ for this case. We also calculated the VACFs for $R = 0.2$ and 0.16 and obtained similar results. These results further strengthen the case for

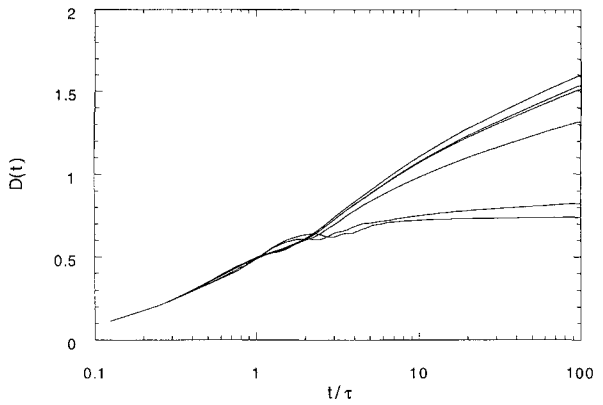

Fig. 10. Time-dependent diffusion coefficient $D(t)$ calculated from the VACFs for $R = 0.42$, 0.4, 0.3, 0.2, 0.17, and 0.125. Curves are, from the top at long times, for $R = 0.125$, 0.17, 0.2, 0.3, 0.4, and 0.42.

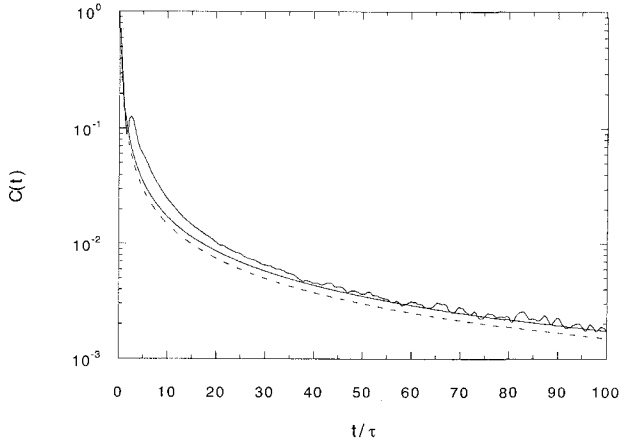

Fig. 11. The VACF $C(t)$ as a function of time in mean free time units for $R=0.17$ with 2.025×10^7 initial conditions sampled. The analytical estimates for the $1/t$ decay $C^{(1)}_{free}(t)$ (a broken curve) and $C^{(2)}_{free}(t)$ (a solid curve) are also plotted.

the $1/t$ decay for the unbounded case, and also strongly supports that the origin of the $1/t$ decay is the long free paths along open channels.

3.3.3.C. 36 Open Channels: $\sqrt{39}/52 \leqslant R < \sqrt{21}/28$. For $\sqrt{39}/52 \leqslant R < \sqrt{21}/28$, we have three sets of twelve open channels, and Fig. 12 shows

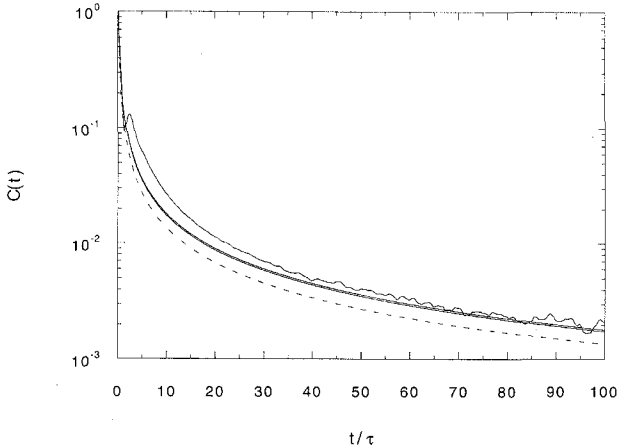

Fig. 12. The VACF $C(t)$ as a function of time in mean free time units for $R=0.125$ with 2.025×10^7 initial conditions sampled. The analytical estimates for the $1/t$ decay $C^{(1)}_{free}(t)$ (a broken curve), $C^{(2)}_{free}(t)$ (the second solid curve), and $C^{(3)}_{free}(t)$ (the solid curve at the top) are also plotted.

that the VACF for $R=0.125$ follows $C^{(3)}_{free}(t)$ given by (3.10) beyond $t \sim 70\tau$. Figure 10 also shows that in this range of time $D(t)$ diverges linearly with $\log_{10}(t)$.

4. CONCLUSIONS

In this paper, we have numerically examined the velocity autocorrelation functions (VACFs) for the periodic Lorentz gas on a triangular lattice. Our main focus has been on the long time tails or decays of the VACFs, especially, their dependence on the radius R of the hard disks on the lattice. Our results are:

(i) For the bounded horizon case ($\sqrt{3}/4 \leqslant R \leqslant 0.5$), the VACF appears to decay exponentially. Presence or absence of the $t^{-1/2}$ pre-factor cannot be determined conclusively from our numerical data, nor can a stretched exponential fit be confirmed or ruled out.

(ii) For the unbounded horizon case ($0 < R < \sqrt{3}/4$), the VACF decays as $1/t$. The calculated VACFs closely follow the analytical formula (3.10) strongly supporting Friedman and Martin's conjecture that the $1/t$ decay is due to the long free paths. The $1/t$ decay is then a consequence of a geometrical feature of the system (namely, open channels), rather than a dynamical property. The emergence of the $1/t$ decay below $R_c = \sqrt{3}/4$ therefore cannot be regarded as a type of critical phenomenon.

In order to observe the $1/t$ decay, we have calculated the VACFs not only over much longer time ranges (*i.e.*, up to $t = 100\tau$) than previously attempted but also for smaller values of R so that the VACFs stay above the level of statistical uncertainty over long times. The logarithmic divergence of the diffusion coefficient $D(t)$ up to time t further supports the $1/t$ decay.

Perhaps needless to say, more analytical work is still needed to clarify the nature of the long time decay of the VACF for both the bounded and unbounded horizon case. For the bounded horizon case, discrimination among purely exponential, exponential with a $t^{-1/2}$ prefactor, or stretched exponential appears to be beyond the capability of this type of numerical calculation. For the unbounded horizon case, we now have a stronger case for the $1/t$ decay, but it is nonetheless highly desirable to have a rigorous proof for it or a rigorous bound for the VACF at long times. Numerically, it may be also possible to clarify the long time behavior of the VNCF for the unbounded case by choosing smaller values of R.

ACKNOWLEDGMENTS

We gratefully acknowledge the financial support provided by Illinois State University through its University Research Grant program. We appreciate several stimulating discussions with Barry Friedman and thank George Skadron for his constant support and encouragement. We also thank Robert D. Young and the Office of Academic Computing at Illinois State University for generously allowing us to use their IBM RS6000s. RFM acknowledges partial support from NSF Grant#ATM-9002447 and CEIS grant #MRT91R0105.

REFERENCES

1. Ya. G. Sinai, Dynamical systems with elastic reflections. Ergodic properties of dispersing billiards, *Russ. Math. Surveys* **25**:137–189 (1970) for the periodic Lorentz gas with a bounded horizon. I. Kubo, *Billiard Problem, Seminar on Probability* **37** (1972) (in Japanese), and *Lect. Notes in Math.* **330**:287 (1973) for the periodic Lorentz gas with an unbounded horizon.
2. G. Gallavotti and D. S. Ornstein, Billiards and Bernoulli schemes, *Commun. Math. Phys.* **38**:83–101 (1974).
3. L. A. Bunimovich and Ya. G. Sinai, Statistical properties of Lorentz gas with periodic configuration of scatterers, *Commun. Math. Phys.* **78**:479–197 (1981). L. A. Bunimovich, Ya. G. Sinai, and N. I. Chernov, Statistical properties of two-dimensional hyperbolic billiards, *Russ. Math. Surveys* **46**:47–106 (1991).
4. G. Casati, G. Comparin, and I. Guarneri, Decay of correlations in certain hyperbolic systems, *Phys. Rev. A* **26**:717–719 (1982).
5. P. L. Garrido and G. Gallavotti, Billiards correlation functions, *J. Stat. Phys.* **76**:549–585 (1994).
6. J. Machta and B. Reinhold, Decay of correlations in the regular Lorentz gas, *J. Stat. Phys.* **42**:949–959 (1986).
7. J. Machta, Power law decay of correlations in a billiard problem, *J. Stat. Phys.* **32**:555–564 (1983).
8. F. Vivaldi, G. Casati, and I. Guarneri, Origin of long-time tails in strongly chaotic systems, *Phys. Rev. Lett.* **51**:727–730 (1983).
9. J.-P. Bouchaud and P. Le Doussal, Numerical study of a d-dimensional periodic Lorentz gas with universal properties, *J. Stat. Phys.* **41**:225–248 (1985).
10. J.-P. Bouchaud and P. Le Doussal, Critical behaviour and intermittency in Sinai's billiard, *Physica D* **20**:335–349 (1986).
11. B. Friedman and R. F. Martin Jr., Decay of the velocity autocorrelation function for the periodic Lorentz gas, *Phys. Lett. A* **105**:23–26 (1984).
12. B. Friedman, The billiard problem, PhD. Thesis, University of Illinois, Physics Department (1985).
13. B. Friedman and R. F. Martin Jr., Behavior of the velocity autocorrelation function for the periodic Lorentz gas, *Physica D* **30**:219–227 (1988).
14. J. Machta and R. Zwanzig, Diffusion in a periodic gas, *Phys. Rev. Lett.* **50**:1959 (1983).
15. L. A. Bunimovich, Decay of correlations in dynamical systems with chaotic behavior, *Zh. Eksp. Teor. Fiz.* **89**:1452–1471 (1985) (*Sov. Phys. JETP* **62**:842–852 (1986)).

16. P. M. Bleher, Statistical properties of two-dimensional periodic Lorentz gas with infinite horizon, *J. Stat. Phys.* **66**:315–373 (1992).
17. A. Zacherl, T. Geisel, J. Nierwetberg, and G. Radons, Power spectra for anomalous diffusion in the extended Sinai billiard, *Phys. Lett. A* **114**:317–321 (1986).
18. N. I. Chernov, Statistical properties of the periodic Lorentz gas. Multidimensional case, *J. Stat. Phys.* **74**:11–53 (1994).
19. C. P. Lowe and A. J. Masters, The long-time behaviour of the velocity autocorrelation function in a Lorentz gas, *Physica A* **195**:149 (1993).